Topical Review

Dynamic clamp: a powerful tool in cardiac electrophysiology

Ronald Wilders

Department of Physiology, Academic Medical Center, University of Amsterdam, Amsterdam, The Netherlands

Dynamic clamp is a collection of closely related techniques that have been employed in cardiac electrophysiology to provide direct answers to numerous research questions regarding basic cellular mechanisms of action potential formation, action potential transfer and action potential synchronization in health and disease. Building on traditional current clamp, dynamic clamp was initially used to create virtual gap junctions between isolated myocytes. More recent applications include the embedding of a real pacemaking myocyte in a simulated network of atrial or ventricular cells and the insertion of virtual ion channels, either simulated in real time or simultaneously recorded from an expression system, into the membrane of an isolated myocyte. These applications have proven that dynamic clamp, which is characterized by the real-time evaluation and injection of simulated membrane current, is a powerful tool in cardiac electrophysiology. Here, each of the three different experimental configurations used in cardiac electrophysiology is reviewed. Also, directions are given for the implementation of dynamic clamp in the cardiac electrophysiology laboratory. With the growing interest in the application of dynamic clamp in cardiac electrophysiology, it is anticipated that dynamic clamp will also prove to be a powerful tool in basic research on biological pacemakers and in identification of specific ion channels as targets for drug development.

(Received 22 June 2006; accepted after revision 21 July 2006; first published online 27 July 2006)
Corresponding author R. Wilders: Department of Physiology, Academic Medical Center, University of Amsterdam, Meibergdreef 15, 1105 AZ Amsterdam, The Netherlands. Email: r.wilders@amc.uva.nl

Traditionally, the electrical properties of excitable cells are assessed with 'current clamp' and 'voltage clamp' protocols. This also holds for today's research in cardiac electrophysiology on single isolated myocytes. Electrical access to the cell interior is obtained through a patch pipette that is used to 'clamp' either current or voltage. In current clamp, a current – typically a rectangular pulse to elicit an action potential – is injected into the myocyte while the (trans)membrane potential is being recorded. In voltage clamp, the membrane potential is kept at a controlled value – typically at constant levels with stepwise changes – using advanced electronic circuitry while the (trans)membrane current is being recorded. Both techniques have contributed to the understanding of the electrical behaviour of the different types of cardiomyocytes. Specifically, the measurement of voltage dependence of individual membrane ionic currents has facilitated the development of detailed mathematical models of the electrical activity of cardiac myocytes. Over the years, voltage clamp protocols have been refined to assess specific properties of membrane current. A particular refinement is the introduction of the 'action potential clamp', in which a prerecorded action potential waveform is used as voltage clamp command potential instead of the traditional step protocols (Doerr *et al.* 1989, 1990).

Recent studies in cardiac electrophysiology (Berecki *et al.* 2005, 2006; Sun & Wang, 2005; Dong *et al.* 2006; Wang *et al.* 2006) demonstrate the growing interest in the application of 'dynamic clamp', which is a less well known but very powerful electrophysiological technique. In general, this technique is used to inject a current into a myocyte in current clamp mode. However, unlike classic current clamp, this current is not known *a priori*. Usually, the current is a function of the free-running membrane potential of the myocyte. Typically, this current mimics the existence of an additional ionic conductance in the cell membrane. The dynamic clamp technique thus operates in a cyclic way: in a continuous loop, the membrane potential is recorded into a computer that calculates the current to be injected and lets the patch clamp amplifier inject this current.

 DOI: 10.1113/jphysiol.2006.115840

In cardiac electrophysiology, the dynamic clamp technique has been used in three different experimental configurations. In this review, each of these configurations is described. Also, directions are given for the implementation of dynamic clamp, which is fundamentally more difficult than traditional voltage clamp or current clamp, because it requires the real-time evaluation and injection of simulated membrane current.

History of dynamic clamp

As briefly discussed before (Wilders, 2005), the dynamic clamp was introduced by Scott (1979) in a study of the bidirectional interaction of two spontaneously beating clusters of embryonic chick ventricular cells, as an extension of his work on phase resetting properties of individual clusters. He designed a system in which two isolated cell clusters not in physical contact with each other could be electrically coupled at any desired value of intercellular resistance by means of an external circuit that continuously applied time-varying currents to each cluster with a sign and magnitude that would have been present if the cells had been physically coupled by gap junctions (or 'nexus'). He impaled each cell cluster with a microelectrode and thus recorded its membrane potential. He then simulated intercellular electrical coupling through gap junctions by creating a physical connection between the two clusters through an analog circuit, named 'Ersatz Nexus'. As illustrated in Fig. 1, the circuit was designed to inject a current into each of the clusters such that they are effectively coupled by a nexus resistance R_N. If $V_{m,1}$ and $V_{m,2}$ are the time-varying membrane potentials of the two clusters, then the time-varying current I_N injected into cluster 2 is given by $I_N = (V_{m,1} - V_{m,2})/R_N$ (Ohm's law), whereas the inverted current is injected into cluster 1. Thus, a 'nexus current' I_N flows between cluster 1 and cluster 2.

Scott also used his Ersatz Nexus to compensate for coupling of an already present *in vivo* nexus by reversing the polarity of the injected currents. Thus, by effectively uncoupling the clusters, he was able to estimate the gap junctional resistance that had developed between two closely apposed clusters. Furthermore, his analog circuitry had a jumper that could be replaced by passive or active devices to simulate an other than strictly ohmic nexus.

About one decade later, Joyner and coworkers independently developed an analog 'coupling clamp' circuit – essentially similar to Scott's Ersatz Nexus – that could be used to simulate gap junctional coupling between two isolated myocytes (Tan & Joyner, 1990; Tan *et al.* 1991; Joyner *et al.* 1991). Shortly after the introduction of the coupling clamp technique in cardiac electrophysiology, similar techniques were independently introduced in neurophysiology by Sharp *et al.* (1992, 1993*a*,*b*) and Robinson & Kawai (1993), named 'dynamic clamp' and 'conductance injection', respectively, with some debate on who was first (Robinson, 1994; Sharp *et al.* 1994), and by Hutcheon *et al.* (1996), named 'reactive current clamp'. Although the dynamic clamp has its origin in cardiac electrophysiology, it is now more common in neurophysiology, where it has particular applications, including the simulation of synaptic activity. These applications have been described in recent reviews with emphasis on neurophysiology (Prinz *et al.* 2004; Goaillard & Marder, 2006).

Dynamic clamp configurations

Based on the experimental setting, three dynamic clamp configurations can be distinguished in cardiac electrophysiology. Each of these configurations is discussed and illustrated below.

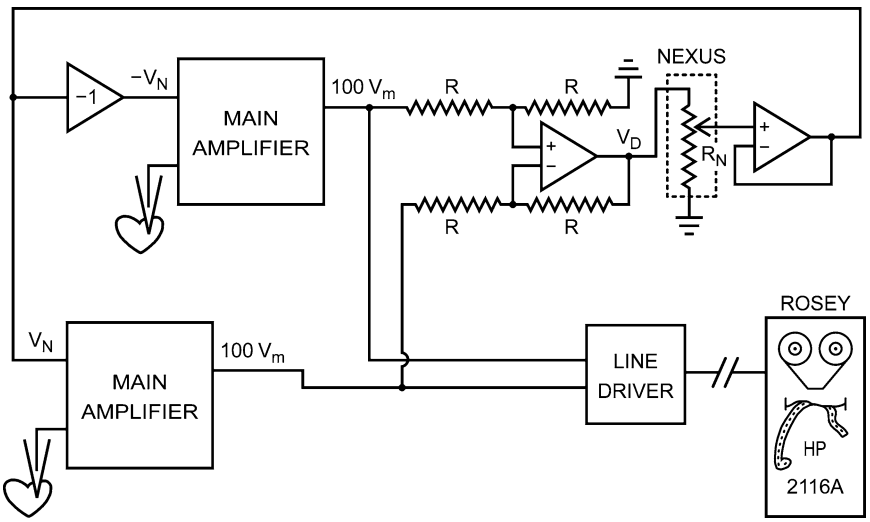

Figure 1. Block diagram of first dynamic clamp setup
Setup used to study the mutual synchronization of two small clusters (~100 μm in diameter) of spontaneously active embryonic chick ventricular cells (Scott, 1979). An analog circuit is used to generate positive and negative command potentials proportional to the difference in membrane potential between the two clusters. These command potentials (V_N and $-V_N$) are sent to the main amplifiers to let them inject a 'nexus current' into each of the clusters such that these are effectively coupled by a nexus resistance R_N. The setup includes a 'minicomputer' (HP 2116A), but its role is limited to recording the membrane potential of each cluster. Redrawn from Fig 2–6 of Scott (1979).

Coupling clamp. Originally, dynamic clamp was used to create electrical connections between myocytes, thus simulating intercellular electrical coupling through gap junctions ('coupling clamp'). Figure 2*A* illustrates how coupling clamp is accomplished. Electrical recordings are made from two isolated myocytes, both in current clamp mode, thus requiring two patch clamp amplifiers. These myocytes can either be in one cell chamber on a single electrophysiological setup or in separate recording chambers on two different electrophysiological setups. The membrane potentials $V_{m,1}$ and $V_{m,2}$ of the two myocytes are sampled into a personal computer. This computer then computes the coupling current I_c flowing from myocyte 1 to myocyte 2, based on $V_{m,1}$ and $V_{m,2}$, and sends command potentials to the amplifiers such that the appropriate current is injected into each of the myocytes, where it contributes to net membrane current and thus affects the membrane potential. Since both $V_{m,1}$ and $V_{m,2}$ may change rapidly with time, this process requires a high update rate, i.e. a small cycle time Δt, typically 100 μs or less.

The coupling clamp configuration of the dynamic clamp technique was used by Verheijck *et al.* (1998) to study the mutual synchronization of two adult pacemaker cells isolated from the rabbit sinoatrial (SA) node. The two cells were simultaneously studied in two separate microscope setups, thus precluding any electrical contact between the cells except that provided by the coupling circuit. To

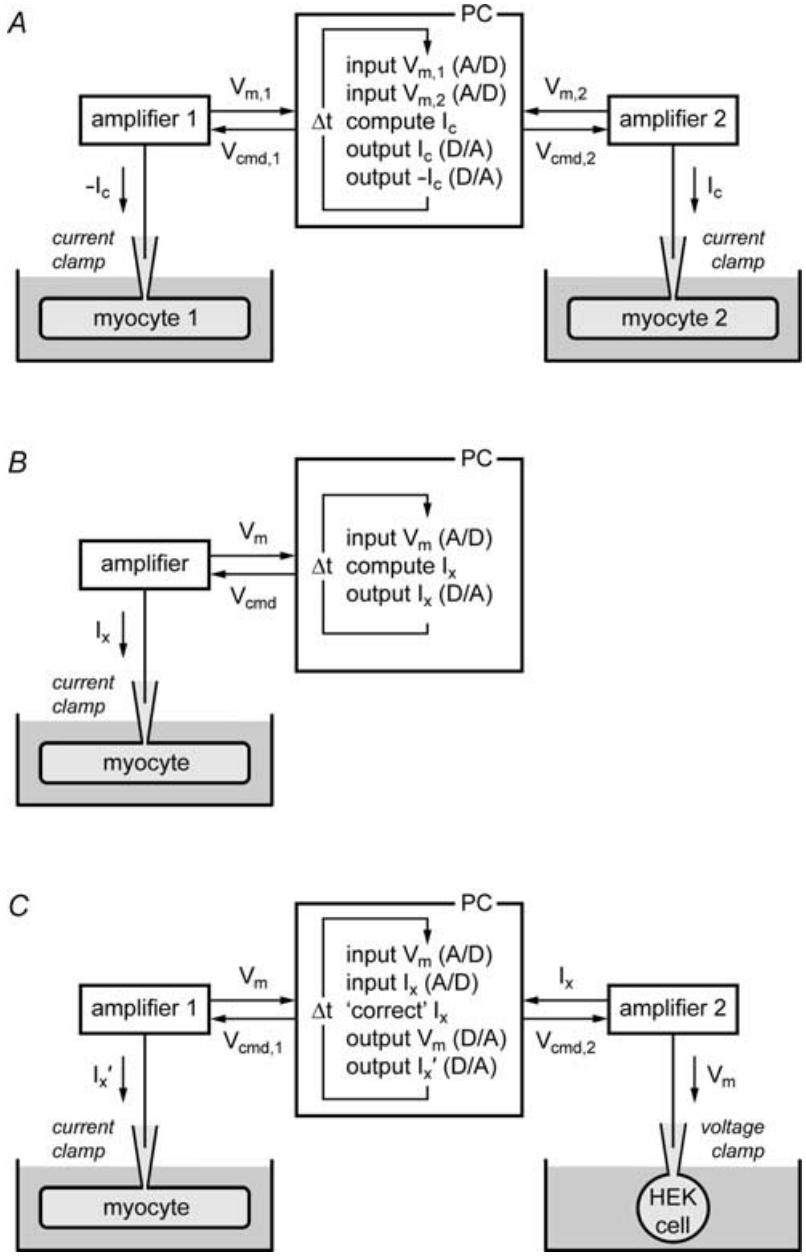

Figure 2. Experimental design of dynamic clamp experiments in cardiac cellular electrophysiology
A, 'coupling clamp' configuration. The membrane potentials of two isolated myocytes ($V_{m,1}$ and $V_{m,2}$), both in current clamp mode, are sampled into a microcomputer (PC) and a coupling current (I_c) is computed, based on $V_{m,1}$ and $V_{m,2}$. Command potentials (V_{cmd}) are then sent to the patch-clamp amplifiers to inject this current into the myocytes as additional membrane current via the recording patch pipettes. The time step for updating input and output values is Δt. *B*, 'model clamp' configuration. The free-running membrane potential of a single isolated myocyte in current clamp mode (V_m) is sampled into a microcomputer (PC). An additional V_m-dependent membrane current (I_x) is computed and injected into the myocyte via the recording patch pipette. *C*, 'dynamic action potential clamp' configuration. The free-running membrane potential of a single isolated myocyte is recorded in current clamp mode and used to voltage clamp a HEK-293 cell, in which a specific ion current is expressed. This ion current (I_x) is fed back to the PC and, after on-line 'correction' (i.e. subtraction of endogenous background current of the HEK cell and appropriate scaling of the remaining current), injected into the myocyte as additional membrane current (I_x').

prevent intracellular dialysis and ensure stable recordings, the amphotericin-perforated patch clamp technique was used to record membrane potentials and currents. Figure 3 shows simultaneous recordings from two SA nodal cells, with the membrane potential recordings of the two cells distinguished by a blue (for cell 1) or red (for cell 2) line. If uncoupled (Fig. 3*A*; zero coupling conductance), the action potentials of the two cells are clearly different in shape, with the spontaneous activity of cell 1 occurring at a shorter interbeat interval (310 ms) than the spontaneous activity of cell 2 (390 ms). The coupling current is, of course, zero (Fig. 3*A*, bottom).

Figure 3*B–D* shows data from the same two cells, using coupling conductance values of 0.2 nS (Fig. 3*B*), 2 nS (Fig. 3*C*) and 10 nS (Fig. 3*D*). Already at 0.2 nS, equivalent to the conductance of only one or a few gap junctional channels, a stable pattern of entrainment of the action potentials of cells 1 and 2 is established. Both at 0.2 and 2 nS, the action potentials of cells 1 and 2 are entrained at a common interbeat interval, but the shapes of the action potentials are still different for cell 1 and cell 2, with cell 2 retaining a more negative maximum diastolic potential and a longer action potential duration (APD): the cells show 'frequency entrainment', but not 'waveform entrainment'. Upon further increasing coupling conductance to 10 nS (Fig. 3*D*), the action potentials of cells 1 and 2 become nearly synchronous, with nearly identical action potential shapes: the cells now show both frequency and waveform entrainment. The common interbeat interval is 333 ms, which is closer to that of the faster beating cell, as expected on theoretical grounds (Verheijck *et al.* 1998). The coupling current, which is plotted as a positive current in the direction from cell 1 to cell 2, increases in magnitude from Fig. 3*B* to Fig. 3*C* to Fig. 3*D* as the coupling conductance increases, but not in a linear fashion because it is not only dependent on coupling conductance but also on driving force, i.e. the difference in membrane potential between the two cells, which decreases with increasing coupling conductance. There is a significant negative component of coupling current (flowing from cell 2 to cell 1) due to the intrinsically longer APD of cell 2. During diastolic depolarization, a sustained

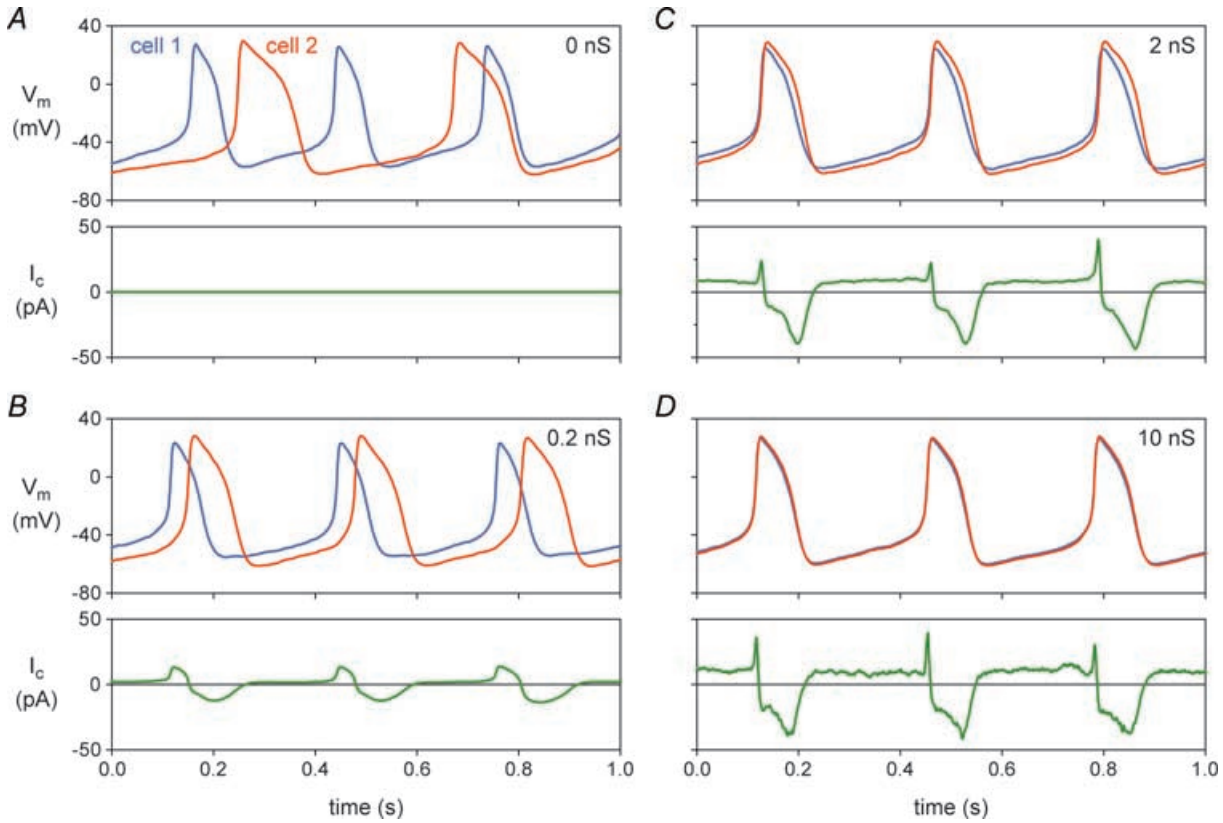

Figure 3. Mutual synchronization of two adult pacemaker cells isolated from the rabbit sinoatrial node
The dynamic clamp technique of Fig. 2*A* was used to introduce an ohmic coupling conductance between the two cells, thus simulating gap junctional conductance. Membrane potential of the two cells (V_m, top) and coupling current flowing in the direction from cell 1 to cell 2 (I_c, bottom). Data from experiment 950803-2 of Verheijck *et al.* (1998). *A*, cells not coupled. *B*, cells coupled by 0.2 nS. *C*, cells coupled by 2 nS. *D*, cells coupled by 10 nS.

'tonic' component of coupling current is flowing from cell 1 to cell 2.

As illustrated in Fig. 3, the dynamic clamp configuration of Fig. 2*A* could be used to study the synchronization process of SA nodal pacemaker cells in detail. Similar experiments were carried out by Spitzer *et al.* (1997), who used an analog coupling clamp circuit to study the mutual entrainment of two adult pacemaker cells isolated from the rabbit atrioventricular (AV) node upon coupling through a 500 MΩ resistance (equivalent to a coupling conductance of 2 nS). To minimize intracellular dialysis, the nystatin-perforated patch clamp technique was used to record the membrane potentials and currents of these nodal cells. In each of the four AV nodal cell pairs studied, the two cells showed frequency entrainment, but not waveform entrainment, upon coupling. Coupling decreased the firing rate of the intrinsically faster beating cell and increased that of the intrinsically slower beating cell to a common intermediate rate. The common firing rate (192 ± 55 beats min^{-1}, mean ± S.D.) was closer to the firing rate of the intrinsically faster beating cell (197 ± 54 beats min^{-1}) than that of the intrinsically slower beating cell (177 ± 54 beats min^{-1}). These values are remarkably similar to those obtained in five SA nodal cell pairs by Verheijck *et al.* (1998). In these cell pairs, the common firing rate was 191 ± 33 beats min^{-1}, whereas the firing rate of the intrinsically faster beating cell was 204 ± 32 beats min^{-1} and that of the intrinsically slower beating cell was 166 ± 39 beats min^{-1}.

Other investigators have used an analog coupling clamp circuit in studies of the modulation of action potential conduction between two isolated guinea pig ventricular myocytes by calcium current (Sugiura & Joyner, 1992), electrotonic modulation of SA node pacemaker activity by atrial muscle (Watanabe *et al.* 1995), interactions between Purkinje and ventricular myocytes (Huelsing *et al.* 1998, 1999, 2000, 2003), beat-to-beat repolarization variability in ventricular myocytes (Zaniboni *et al.* 2000), and effects of transient outward current inhibition on conduction between ventricular myocytes (Huelsing *et al.* 2001). In several of these studies, one of the myocytes of Fig. 2*A* was replaced with an RC circuit as a model of an atrial or ventricular myocyte.

Model clamp. Dynamic clamp may also be used to simulate the presence of an additional conductance in the membrane of a single isolated myocyte. In this configuration (Fig. 2*B*), the membrane potential V_m of the myocyte is continuously sampled into a personal computer, which calculates the V_m-dependent current I_x and sends a command potential to the amplifier to inject this current into the myocyte. This configuration has been referred to as 'model clamp' (Wilders *et al.* 1996*b*), because a model-based current is injected into the myocyte. In neurophysiology, it has been named 'model reference current injection' (Butera *et al.* 2001; Raikov *et al.* 2004).

A relatively simple application of the model clamp technique is shown in Fig. 4. Verkerk *et al.* (2000) used this technique to inject an ohmic current with a reversal potential of −40 mV and an adjustable conductance G_x into an isolated human ventricular myocyte. This current represented the 'injury current' flowing from normal myocardium to ischaemic tissue, which is known to contain inexcitable cells that are depolarized to about −40 mV (Downar *et al.* 1977). In the absence of injury current, i.e. with $G_x = 0$ (Fig. 4, green lines), the ventricular myocyte has a resting potential of −82 mV and an APD of ∼420 ms. Upon the introduction of injury current with a conductance of 10 nS, the APD shortens to ∼180 ms and the resting potential depolarizes by 3–4 mV (Fig. 4, blue lines). Increasing the injury conductance to 20 nS induces further APD shortening and depolarization of the resting potential (Fig. 4, red lines). However, the injury current did not induce afterdepolarizations, in contrast with postulations made in previous studies (see

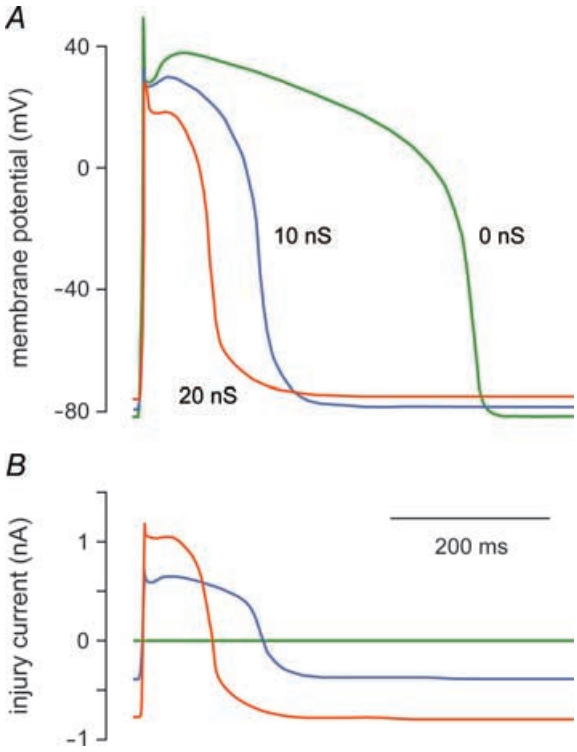

Figure 4. Effect of simulated 'injury current' on the human left ventricular action potential
The dynamic clamp technique of Fig. 2*B* was used to inject a time-varying current into an isolated human left ventricular myocyte. This current was computed as an ohmic current with a reversal potential of −40 mV and a conductance of 0, 10 or 20 nS, as indicated, and represents the 'injury current' that flows from normal myocardium to a depolarized ischaemic region. Data from Verkerk *et al.* (2000). *A*, superimposed action potentials of the myocyte. *B*, injected 'injury current'. The myocyte was paced at 1 Hz.

Janse & Wit, 1989). These only occurred if its reversal potential was set to less negative potentials (Verkerk *et al.* 2000). Similar findings had previously been made in guinea pig ventricular myocytes by Kumar & Joyner (1994).

The model clamp configuration of Fig. 2*B* has also been used to introduce a specific membrane current into cardiomyocytes, e.g. stretch-activated current in rat atrial cells (Wagner *et al.* 2004) and transient outward current in guinea pig and canine endocardial ventricular myocytes (Sun & Wang, 2005; Dong *et al.* 2006). This current is then computed in real time based on a mathematical model of voltage and time dependence of the current. However, the current that is injected into the myocyte can also represent gap junctional current flow to a second myocyte, with both junctional current and the second myocyte simulated in real time (Joyner *et al.* 1996, 1998; Kumar *et al.* 1996; Wagner *et al.* 1997, 2000; Wilders *et al.* 1996*a*,*b*, 1999). The geometry can even be made more complex with the real myocyte embedded in a virtual network of atrial or ventricular myocytes (Wagner *et al.* 1999; Joyner *et al.* 2000; Wang *et al.* 2000). The injected current is then the net current flowing between the real myocyte and the virtual myocytes to which it is connected.

Model clamp has also proven useful in studies of the differences in bursting properties between isolated mouse pancreatic β-cells and intact islets, with the more stochastic electrical activity of isolated β-cells producing faster and less regular intracellular calcium oscillations (Zhang *et al.* 2003). Introduction of a very small slowly activating inward current into isolated β-cells converted the electrical activity of spiking or fast-bursting β-cells to a more islet-like electrical pattern, resulting in more regular and islet-like intracellular calcium oscillations. Similarly, model clamp may prove useful in studies of isolated cardiac pacemaker cells, where the stochastic nature of ion channels influences diastolic depolarization and associated calcium oscillations.

Dynamic action potential clamp. A novel and promising application of the dynamic clamp technique is 'dynamic action potential clamp' (Berecki *et al.* 2005, 2006). In this configuration (Fig. 2*C*), which was designed to provide a more physiological setting than traditional action potential clamp with a prerecorded action potential, a native ionic current of a cardiomyocyte is pharmacologically blocked and replaced with wild-type or mutant current recorded from a HEK-293 cell that is voltage-clamped by the free-running action potential of the myocyte. In their initial study, Berecki *et al.* (2005) used this technique to investigate the effects of a long-QT syndrome-related mutation in the human *ether-à-go-go*-related gene (*HERG*), which encodes the rapid component of the cardiac delayed rectifier potassium current (I_{Kr}). In this case, the myocyte of Fig. 2*C* was an isolated rabbit ventricular myocyte with its native I_{Kr} blocked by E-4031, whereas the HEK-293 cell was transiently transfected with wild-type or R56Q mutant *HERG* cDNA and thus expressed wild-type or mutant HERG current. In this experimental setting, the wild-type or mutant HERG channels are allowed to follow the natural time course of an action potential (through V_m), upon being simultaneously allowed to contribute current for the generation of this action potential as if they were incorporated into the myocyte (through injection of the HERG current into the myocyte). This is illustrated in Fig. 5, which shows action potentials from the same myocyte generated with the contribution of either wild-type or mutant HERG current (blue and red traces, respectively), obtained by subsequently coupling the myocyte to a HEK-293 cell expressing wild-type current and a HEK-293 cell expressing mutant current. Wild-type and mutant HERG current were both scaled down to produce a HERG current density comparable to the native I_{Kr} density of the myocyte, as estimated from the E-4031-sensitive current. This scaling procedure seemed appropriate because the R56Q mutation is associated with

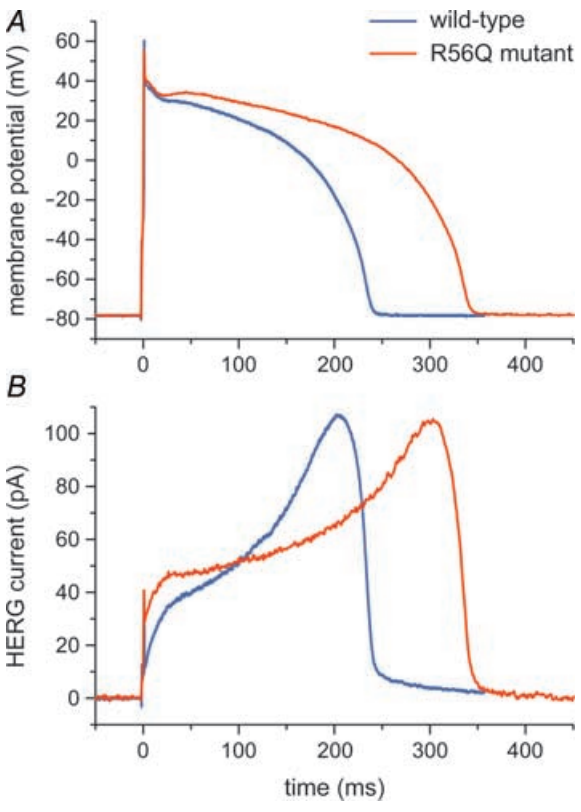

Figure 5. Effect of a HERG channel mutation probed with dynamic action potential clamp
The native delayed rectifier potassium current (I_{Kr}) of an isolated rabbit left ventricular myocyte was blocked by E-4031 and replaced with either wild-type or R56Q mutant HERG current expressed in a HEK-293 cell using the dynamic clamp technique of Fig. 2*C* (Berecki *et al.* 2005). *A*, superimposed action potentials of the isolated myocyte, which was paced at 1 Hz. *B*, associated HERG current.

altered gating properties rather than impaired trafficking from the endoplasmic reticulum to the cell membrane.

The experiment of Fig. 5 directly demonstrates that the R56Q mutation results in significant action potential prolongation (Fig. 5*A*) and provides insights in the underlying mechanism (Fig. 5*B*). Note that this action potential prolongation occurs despite the larger initial HERG current in the mutant case. This demonstrates that the change in action potential profile is not only the result of changes in HERG current but also of changes in other membrane currents through their dependence on membrane potential. The latter changes can be assessed using the recorded action potentials as voltage waveforms in traditional action potential clamp experiments or computer simulations.

In their subsequent study, Berecki *et al.* (2006) used the dynamic action potential clamp technique to investigate the effects of the Y1795C and A1330P long-QT syndrome-related mutations in the *SCN5A* gene, which encodes the pore-forming subunit of the cardiac sodium channel. In this case, the isolated myocyte of Fig. 2*C* was replaced with a real-time simulation of a human ventricular myocyte. They demonstrated that the sodium channel mutations resulted in significant action potential prolongation and in a significantly steeper APD–frequency relationship. Also, they showed that the action potential prolongation was more pronounced for the mid-myocardial cell type, resulting in increased APD dispersion. Furthermore, a 2 s pause following rapid pacing resulted in distorted action potential morphology associated with beat-to-beat fluctuations of sodium current. Thus, these dynamic action potential clamp experiments directly demonstrated the arrhythmogenic nature of long-QT syndrome-related mutations in the *SCN5A* gene.

Setting up dynamic clamp

The value of the dynamic clamp technique in cardiac electrophysiology is becoming widely appreciated. However, implementation of the technique is not straightforward. Therefore, some guidelines for setting up dynamic clamp are given below.

Hardware implementations. If the purpose of dynamic clamp is to compute and inject ohmic current, one may prefer to use custom analog circuitry, similar to that of Scott (1979) and Tan & Joyner (1990). For applications beyond computing and injecting ohmic current there are two commercially available dynamic clamp systems. These are the ITC-18 data acquisition interface (Instrutech Corporation, Port Washington, NY, USA) and the Synaptic Module 1 (SM-1) conductance injection amplifier (Cambridge Conductance, Cambridge, UK). Both are hardware implementations with built-in analog devices, primarily designed to create artificial synapses by injecting a current into a current-clamped neurone based on specific equations that include the membrane potential of the neurone and the conductance and reversal potential of the current (Robinson, 1999). A particular advantage of these hardware implementations is the high speed at which they operate, with a minimal input to output delay of 20 μs.

Software implementations. As an alternative to using dedicated hardware, one may use hardware that is available in most cardiac electrophysiology laboratories, i.e. a PC equipped with a multifunction data acquisition board, and use dedicated software to turn this hardware into a dynamic clamp system. Once running, such a computer-controlled system combines ease of use and high flexibility and is therefore the system of first choice for most applications. Dynamic clamp software is not commercially available, but several research groups have made their custom software publicly available (Table 1). With the exception of 'DynaClamp' (Berecki *et al.* 2005, 2006), all software was mainly developed for use in neurophysiology.

As illustrated in Fig. 2, dynamic clamp software should be able to continuously sample one or two analog signals, carry out computations based on the acquired data, and send out one or two analog signals based on the outcome of these computations. This implies that, in contrast with traditional data acquisition software, data buffering is not useful with dynamic clamp because individual samples are processed immediately after they are acquired. With today's computer processor speed the limiting factor for the overall speed (update rate) of the dynamic clamp system is the rate of signal input and output operations, even if complex mathematical models are used in the computations of the current to be injected. It is therefore advisable to use a data acquisition board that allows fast analog-to-digital (A/D) and digital-to-analog (D/A) conversions. At the same time, given the feedback between current and voltage inherent to dynamic clamp, it is important to select a board with high-precision, typically 16-bit, A/D and D/A conversions, thereby minimizing the errors introduced by discretization of current and voltage. This is even more important if the current under investigation has a wide dynamic range such as the fast sodium current, with the late component flowing during the vulnerable action potential plateau being approximately 1000 times smaller than the current flowing during the action potential upstroke (Berecki *et al.* 2006). With proper selection of hardware and software, an update rate of 10–50 kHz, corresponding with a cycle time of 20–100 μs, can be achieved.

With regard to the operating system, the available software either runs on Windows or real-time Linux (RT-Linux; Barabanov & Yodaiken, 1997) -based systems.

Table 1. Publicly available dynamic clamp software

Name	Reference	Configuration*	Platform	Notes
Dynamic clamp	Manor & Nadim (2001)	A,B	Windows	Available at http://stg.rutgers.edu/ Requires National Instruments data acquisition board
DynClamp2	Pinto *et al.* (2001)	A,B	Windows	Available at http://inls.ucsd.edu/~rpinto/ Requires Axon Instruments Digidata 1200A data acquisition board
Real-time Linux dynamic controller (RTLDC)	Dorval *et al.* (2001)	B	RT-Linux	Available at http://www.bu.edu/ndl/
Model reference current injection (MRCI)	Butera *et al.* (2001), Raikov *et al.* (2004)	B	RT-Linux	Available at http://www.neuro.gatech.edu/mrci/
G-clamp	Kullman *et al.* (2004)	B	Windows	Available at http://hornlab.neurobio.pitt.edu Requires National Instruments LabVIEW-RT hardware and software components
Advanced dynamic clamp	Muñiz *et al.* (2005)	B	RT-Linux	Available at http://www.ii.uam.es/~gnb/adclamp
DynaClamp	Berecki *et al.* (2005, 2006)	C	RT-Linux	Available at http://www.physiol.med.uu.nl/dynaclamp/

*A, B and C refer to the dynamic clamp configurations of Fig. 2*A*, *B* and *C*, respectively.

Windows-based software seems attractive for its ease of use, but has particular disadvantages. As listed in Table 1, all software running on Windows systems requires specific hardware components. More importantly, as set out in detail by Butera *et al.* (2001) and Dorval *et al.* (2001), Windows is not well suited for running time-critical applications like dynamic clamp. There is no guarantee that voltage and current are continuously updated with the desired small cycle time Δt (cf. Fig. 2) and with minimal jitter (step-to-step variation in actual Δt). In the 'G-clamp' software by Kullman *et al.* (2004) this has been overcome by using the Windows computer as a host for an embedded microprocessor that runs a real-time operating system and a multifunction data acquisition board. Thus, it has the disadvantage of requiring additional hardware. Also, it requires the full National Instruments LabVIEW programming environment as well as the LabVIEW-RT real-time module (National Instruments, Austin, TX, USA).

All RT-Linux-based dynamic clamp software requires a PC running the Linux operating system with one of the publicly available hard real-time extensions, e.g. RTAI (Real Time Application Interface; Department of Aerospace Engineering, Polytechnic Institute of Milan, Milan, Italy) or RTLinuxFree (FSMLabs, Socorro, NM, USA). Essentially, as set out in detail by Christini *et al.* (1999), RT-Linux is a minimal operating system that runs two processes, i.e. a real-time process (top priority, guaranteed timing) and the standard Linux operating system (low priority, absolutely interruptible by the real-time process). The dynamic clamp software has a real-time part that ensures that all time-critical operations are executed in real time, and a non-real-time part that provides for user-control of the program, such as changing parameters and logging of data. To communicate with the data acquisition board, the software uses an open-source project known as Comedi (Control and Measurement Device Interface) that provides the software to control a wide variety of common data acquisition boards, including most of the boards used by cardiac electrophysiologists.

If setting up a computer-controlled dynamic clamp system, an RT-Linux-based system is recommended. First, the RT-Linux operating system and the Comedi library together provide a robust and inexpensive platform that is well-suited for running dynamic clamp software and will probably be available for many years to come. Second, ready-to-use software is available for this platform as well as source code that may function as a template for writing custom dynamic clamp software. Third, developers of the RTLDC and MRCI dynamic clamp software (Table 1) are involved in the 'Real-Time eXperiment Interface' (RTXI) project, which is a collaborative open-source software development project aimed at producing an RT-Linux-based software system for hard real-time data acquisition and control applications in biological research.

Limitations

Like any experimental technique, dynamic clamp comes with limitations. An important limitation is that the dynamic clamp mimics the electrical effects of a specific ionic current, but not necessarily its signal conduction effects, because the injected current enters the cell through the patch pipette rather than through real ion channels.

Thus, there may be differences in ions carrying the current and in local changes in ion concentration. This limitation can, however, be beneficial if one aims to study electrical effects in isolation. Second, the dynamic clamp can induce errors through latency, i.e. the time lag between acquiring voltage and applying the current based on that voltage. A third limitation is that dynamic clamp, in particular in its model clamp configuration (Fig. 2*B*), relies on a mathematical description of ion current. A related particular limitation of the dynamic action potential clamp configuration (Fig. 2*C*) is that ion channels may behave differently, e.g. show different gating properties, in an expression system. Another particular limitation of the dynamic action potential clamp configuration is that the expressed current has to be scaled before injection into the myocyte, with improper determination of the scaling factor as a potential source of errors. The required scaling can, however, also be beneficial in separating the effects of altered gating properties and impaired trafficking. This may prove especially useful when studying ion channel mutations with opposing effects of alterations in gating properties and alterations in channel expression (e.g. Paulussen *et al.* 2005). Finally, a practical limitation is that dynamic clamp may require simultaneous stable recordings from two myocytes or from one myocyte and one transfected cell (Fig. 2*A* and *C*, respectively).

Concluding remarks

Dynamic clamp has been used to provide direct answers to numerous research questions regarding basic cellular mechanisms of cardiac action potential formation, action potential transfer and action potential synchronization in health and disease. Starting with the synchronization experiments by Scott (1979), the dynamic clamp has evolved to a set of elegant techniques that allow detailed studies of the role of specific ionic currents. With the growing interest in the application of dynamic clamp in cardiac electrophysiology, it is anticipated that dynamic clamp will prove a powerful tool in basic research on biological pacemakers and in identification of specific ion channels as targets for drug development.

References

Barabanov M & Yodaiken V (1997). Introducing real-time Linux. *Linux J* **34**, 19–23.

Berecki G, Zegers JG, Bhuiyan ZA, Verkerk AO, Wilders R & van Ginneken ACG (2006). Long-QT syndrome-related sodium channel mutations probed by the dynamic action potential clamp technique. *J Physiol* **570**, 237–250.

Berecki G, Zegers JG, Verkerk AO, Bhuiyan ZA, de Jonge B, Veldkamp MW, Wilders R & van Ginneken ACG (2005). HERG channel (dys)function revealed by dynamic action potential clamp technique. *Biophys J* **88**, 566–578.

Butera RJ Jr, Wilson CG, Delnegro CA & Smith JC (2001). A methodology for achieving high-speed rates for artificial conductance injection in electrically excitable biological cells. *IEEE Trans Biomed Eng* **48**, 1460–1470.

Christini DJ, Stein KM, Markowitz SM & Lerman BB (1999). Practical real-time computing system for biomedical experiment interface. *Ann Biomed Eng* **27**, 180–186.

Doerr T, Denger R, Doerr A & Trautwein W (1990). Ionic currents contributing to the action potential in single ventricular myocytes of the guinea pig studied with action potential clamp. *Pflugers Arch* **416**, 230–237.

Doerr T, Denger R & Trautwein W (1989). Calcium currents in single SA nodal cells of the rabbit heart studied with action potential clamp. *Pflugers Arch* **413**, 599–603.

Dong M, Sun X, Prinz AA & Wang H-S (2006). Effect of simulated I_{to} on guinea pig and canine ventricular action potential morphology. *Am J Physiol Heart Circ Physiol* **291**, H631–H637.

Dorval AD, Christini DJ & White JA (2001). Real-time Linux dynamic clamp: a fast and flexible way to construct virtual ion channels in living cells. *Ann Biomed Eng* **29**, 897–907.

Downar E, Janse MJ & Durrer D (1977). The effect of acute coronary artery occlusion on subepicardial transmembrane potentials in the intact porcine heart. *Circulation* **56**, 217–224.

Goaillard J-M & Marder E (2006). Dynamic clamp analyses of cardiac, endocrine, and neural function. *Physiology* **21**, 197–207.

Huelsing DJ, Pollard AE & Spitzer KW (2001). Transient outward current modulates discontinuous conduction in rabbit ventricular cell pairs. *Cardiovasc Res* **49**, 779–789.

Huelsing DJ, Spitzer KW, Cordeiro JM & Pollard AE (1998). Conduction between isolated rabbit Purkinje and ventricular myocytes coupled by a variable resistance. *Am J Physiol* **274**, H1163–H1173.

Huelsing DJ, Spitzer KW, Cordeiro JM & Pollard AE (1999). Modulation of repolarization in rabbit Purkinje and ventricular myocytes coupled by a variable resistance. *Am J Physiol* **276**, H572–H581.

Huelsing DJ, Spitzer KW & Pollard AE (2000). Electrotonic suppression of early afterdepolarizations in isolated rabbit Purkinje myocytes. *Am J Physiol Heart Circ Physiol* **279**, H250–H259.

Huelsing DJ, Spitzer KW & Pollard AE (2003). Spontaneous activity induced in rabbit Purkinje myocytes during coupling to a depolarized model cell. *Cardiovasc Res* **59**, 620–627.

Hutcheon B, Miura RM & Puil E (1996). Models of subthreshold membrane resonance in neocortical neurons. *J Neurophysiol* **76**, 698–714.

Janse MJ & Wit AL (1989). Electrophysiological mechanisms of ventricular arrhythmias resulting from myocardial ischemia and infarction. *Physiol Rev* **69**, 1049–1169.

Joyner RW, Kumar R, Golod DA, Wilders R, Jongsma HJ, Verheijck EE, Bouman LN, Goolsby WN & van Ginneken ACG (1998). Electrical interactions between a rabbit atrial cell and a nodal cell model. *Am J Physiol* **274**, H2152–H2162.

Joyner RW, Kumar R, Wilders R, Jongsma HJ, Verheijck EE, Golod DA, van Ginneken ACG, Wagner MB & Goolsby WN (1996). Modulating L-type calcium current affects discontinuous cardiac action potential conduction. *Biophys J* **71**, 237–245.

Joyner RW, Sugiura H & Tan RC (1991). Unidirectional block between isolated rabbit ventricular cells coupled by a variable resistance. *Biophys J* **60**, 1038–1045.

Joyner RW, Wang YG, Wilders R, Golod DA, Wagner MB, Kumar R & Goolsby WN (2000). A spontaneously active focus drives a model atrial sheet more easily than a model ventricular sheet. *Am J Physiol Heart Circ Physiol* **279**, H752–H763.

Kullmann PH, Wheeler DW, Beacom J & Horn JP (2004). Implementation of a fast 16-bit dynamic clamp using LabVIEW-RT. *J Neurophysiol* **91**, 542–554.

Kumar R & Joyner RW (1994). An experimental model of the production of early afterdepolarizations by injury current from an ischemic region. *Pflugers Arch* **428**, 425–432.

Kumar R, Wilders R, Joyner RW, Jongsma HJ, Verheijck EE, Golod DA, van Ginneken ACG & Goolsby WN (1996). Experimental model for an ectopic focus coupled to ventricular cells. *Circulation* **94**, 833–841.

Manor Y & Nadim F (2001). Frequency regulation demonstrated by coupling a model and a biological neuron. *Neurocomputing* **38–40**, 269–278.

Muñiz C, Arganda S, de Borja Rodríguez F & de Polavieja GG (2005). Realistic stimulation through advanced dynamic-clamp protocols. *Lect Notes Comput Sc* **3561**, 95–105.

Paulussen ADC, Raes A, Jongbloed RJ, Gilissen RAHJ, Wilde AAM, Snyders DJ, Smeets HJM & Aerssens J (2005). HERG mutation predicts short QT based on channel kinetics but causes long QT by heterotetrameric trafficking deficiency. *Cardiovasc Res* **67**, 467–475.

Pinto RD, Elson RC, Szücs A, Rabinovich MI, Selverston AI & Abarbanel HDI (2001). Extended dynamic clamp: controlling up to four neurons using a single desktop computer and interface. *J Neurosci Meth* **108**, 39–48.

Prinz AA, Abbott LF & Marder E (2004). The dynamic clamp comes of age. *Trends Neurosci* **27**, 218–224.

Raikov I, Preyer A & Butera RJ (2004). MRCI: a flexible real-time dynamic clamp system for electrophysiology experiments. *J Neurosci Meth* **30**, 109–123.

Robinson HPC (1994). Conductance injection. *Trends Neurosci* **17**, 147.

Robinson HPC (1999). Analog circuits for injecting time-varying linear and non-linear (NMDA-type) conductances into neurons. *J Physiol* **518.P**, 9–10*P*.

Robinson HPC & Kawai N (1993). Injection of digitally synthesized synaptic conductance transients to measure the integrative properties of neurons. *J Neurosci Meth* **49**, 157–165.

Scott S (1979). Stimulation simulations of young yet cultured beating hearts. PhD Thesis, State University of New York at Buffalo.

Sharp AA, Abbott LF & Marder E (1992). Artificial electrical synapses in oscillatory networks. *J Neurophysiol* **67**, 1691–1694.

Sharp AA, O'Neil MB, Abbott LF & Marder E (1993*a*). Dynamic clamp: computer-generated conductances in real neurons. *J Neurophysiol* **69**, 992–995.

Sharp AA, O'Neil MB, Abbott LF & Marder E (1993*b*). The dynamic clamp: artificial conductances in biological neurons. *Trends Neurosci* **16**, 389–394.

Sharp AA, O'Neil MB, Abbott LF & Marder E (1994). Conductance injection – Reply. *Trends Neurosci* **17**, 147–148.

Spitzer KW, Sato N, Tanaka H, Firek L, Zaniboni M & Giles WR (1997). Electrotonic modulation of electrical activity in rabbit atrioventricular node myocytes. *Am J Physiol* **273**, H767–H776.

Sugiura H & Joyner RW (1992). Action potential conduction between guinea pig ventricular cells can be modulated by calcium current. *Am J Physiol* **263**, H1591–H1604.

Sun X & Wang H-S (2005). Role of the transient outward current (I_{to}) in shaping canine ventricular action potential – a dynamic clamp study. *J Physiol* **564**, 411–419.

Tan RC & Joyner RW (1990). Electrotonic influences on action potentials from isolated ventricular cells. *Circ Res* **67**, 1071–1081.

Tan RC, Osaka T & Joyner RW (1991). Experimental model of effects on normal tissue of injury current from ischemic region. *Circ Res* **69**, 965–974.

Verheijck EE, Wilders R, Joyner RW, Golod DA, Kumar R, Jongsma HJ, Bouman LN & van Ginneken ACG (1998). Pacemaker synchronization of electrically coupled rabbit sinoatrial node cells. *J Gen Physiol* **111**, 95–112.

Verkerk AO, Veldkamp MW, de Jonge N, Wilders R & van Ginneken ACG (2000). Injury current modulates afterdepolarizations in single human ventricular cells. *Cardiovasc Res* **47**, 124–132.

Wagner MB, Golod DA, Wilders R, Verheijck EE, Joyner RW, Kumar R, Jongsma HJ, van Ginneken ACG & Goolsby WN (1997). Modulation of propagation from an ectopic focus by electrical load and by extracellular potassium. *Am J Physiol* **272**, H1759–H1769.

Wagner MB, Kumar R, Joyner RW & Wang Y (2004). Induced automaticity in isolated rat atrial cells by incorporation of a stretch-activated conductance. *Pflugers Arch* **447**, 819–829.

Wagner MB, Namiki T, Wilders R, Joyner RW, Jongsma HJ, Verheijck EE, Kumar R, Golod DA, Goolsby WN & van Ginneken ACG (1999). Electrical interactions among real cardiac cells and cell models in a linear strand. *Am J Physiol* **276**, H391–H400.

Wagner MB, Wang YG, Kumar R, Golod DA, Goolsby WN & Joyner RW (2000). Measurements of calcium transients in ventricular cells during discontinuous action potential conduction. *Am J Physiol Heart Circ Physiol* **278**, H444–H451.

Wang Y, Cheng J, Joyner RW, Wagner MB & Hill JA (2006). Remodeling of early-phase repolarization: a mechanism of abnormal impulse conduction in heart failure. *Circulation* **113**, 1849–1856.

Wang YG, Kumar R, Wagner MB, Wilders R, Golod DA, Goolsby WN & Joyner RW (2000). Electrical interactions between a real ventricular cell and an anisotropic two-dimensional sheet of model cells. *Am J Physiol Heart Circ Physiol* **278**, H452–H460.

Watanabe EI, Honjo H, Anno T, Boyett MR, Kodama I & Toyama J (1995). Modulation of pacemaker activity of sinoatrial node cells by electrical load imposed by an atrial cell model. *Am J Physiol* **269**, H1735–H1742.

Wilders R (2005). 'Dynamic clamp' in cardiac electrophysiology. *J Physiol* **566**, 641.

Wilders R, Kumar R, Joyner RW, Jongsma HJ, Verheijck EE, Golod D, van Ginneken ACG & Goolsby WN (1996*a*). Action potential conduction between a ventricular cell model and an isolated ventricular cell. *Biophys J* **70**, 281–295.

Wilders R, Verheijck EE, Joyner RW, Golod DA, Kumar R, van Ginneken ACG, Bouman LN & Jongsma HJ (1999). Effects of ischemia on discontinuous action potential conduction in hybrid pairs of ventricular cells. *Circulation* **99**, 1623–1629.

Wilders R, Verheijck EE, Kumar R, Goolsby WN, van Ginneken ACG, Joyner RW & Jongsma HJ (1996*b*). Model clamp and its application to synchronization of rabbit sinoatrial node cells. *Am J Physiol* **271**, H2168–H2182.

Zaniboni M, Pollara AE, Yang L & Spitzer KW (2000). Beat-to-beat repolarization variability in ventricular myocytes and its suppression by electrical coupling. *Am J Physiol Heart Circ Physiol* **278**, H667–H687.

Zhang M, Goforth P, Bertram R, Sherman A & Satin L (2003). The Ca^{2+} dynamics of isolated mouse β-cells and islets: implications for mathematical models. *Biophys J* **84**, 2852–2870.